

# Fabrication of microfluidic devices using MeV ion beam Programmable Proximity Aperture Lithography (PPAL)

S. Gorelick<sup>a,\*</sup>, N. Puttaraksa<sup>a,b</sup>, T. Sajavaara<sup>a</sup>, M. Laitinen<sup>a</sup>, S. Singkarat<sup>b</sup>, H.J. Whitlow<sup>a</sup>

<sup>a</sup> Department of Physics, University of Jyväskylä, P.O. Box 35 (FL), FIN 40014 Jyväskylä, Finland

<sup>b</sup> Fast Neutron Research Facility, Department of Physics, Chiang Mai University, Chiang Mai 50200, Thailand

Available online 7 March 2008

## Abstract

MeV ion beam lithography is a direct writing technique capable of producing microfluidic patterns and lab-on-chip devices with straight walls in thick resist films. In this technique a small beam spot of MeV ions is scanned over the resist surface to generate a latent image of the pattern. The microstructures in resist polymer can be then revealed using a chemical developer that removes exposed resist, while leaving unexposed resist unaffected. In our system the size of the rectangular beam spot is programmably defined by two L-shaped tantalum blades with well-polished edges. This allows rapid exposure of entire rectangular pattern elements up to  $500 \times 500 \mu\text{m}$  in one step. By combining different dimensions of the defining aperture with the sample movements relative to the beam spot, entire fluidic patterns with large reservoirs and narrow flow channels can be written over large areas in short time. Fluidic patterns were written in PMMA using 56 MeV  $^{14}\text{N}^{3+}$  and a 3 MeV  $^4\text{He}^{2+}$  beams from K130 cyclotron and a 1.7 MV Pelletron accelerators, respectively, at the University of Jyväskylä Accelerator Laboratory. The patterns were characterized using SEM, and the factors affecting patterns quality are discussed.

© 2008 Elsevier B.V. All rights reserved.

PACS: 29.20.Ba; 29.20.dg; 41.85.Si; 87.85.Lf; 87.85.Ox; 61.80.Jh

Keywords: MeV ion beam lithography; Heavy ion beam lithography; Single ion-tracks; Proximity aperture; Microfluidic device; Cell-growth substrate; PMMA

## 1. Introduction

Microfluidic devices become increasingly relevant in biomedical applications and research. Such devices can be effectively used to manipulate and navigate selected cells to a desired location on a patterned substrate [1], to sort different types of cells [2], to evaluate membrane electrical properties of single cells to determine their viability [3], to detect, sequence and size DNA molecules [4–6], and for other numerous applications [7,8]. For our bone–tissue research at cellular and sub-cellular levels [9] we are interested in rapid production of cell-growth substrates and

microfluidic devices in thick polymer films with a large number of pattern elements covering large areas. For this purpose we have constructed a lithography facility for writing patterns with MeV ion beams in polymer resist films, e.g. PMMA [10].

The MeV ion beam writing is a rapidly evolving lithography technique which has proven its capability to produce 3D structures in thick resists with extraordinarily high line-width to resist-thickness aspect ratio ( $>100$ ), nanometre feature sizes ( $\sim 20 \text{ nm}$ ), and a high degree of smoothness [12–14].

MeV ion beam writing, such as Proton Beam Writing (PBW) [12–14], is similar to electron beam lithography (EBL). An ion beam (typically protons or alpha particles) from an accelerator is focused into a small beam spot which is magnetically scanned over the resist surface to

\* Corresponding author. Tel.: +358 14 260 2399; fax: +358 14 260 2351.  
E-mail address: [gorelicks@jyu.fi](mailto:gorelicks@jyu.fi) (S. Gorelick).

generate a latent image of the desired pattern. The advantage of MeV ions, as opposed to electrons, is that MeV ions can penetrate deep into the resist along a straight path and with minimal scattering. In an alternative approach, rather than focusing the MeV ion beam and scanning it across the resist, the target is moved relative to a small beam spot defined by collimators [15,16]. In Programmable Proximity Aperture Lithography (PPAL) used in our system, the size of the rectangular beam spot of MeV ions is programmably defined by two L-shaped tantalum blades (each blade is made of two 100  $\mu\text{m}$  Ta sheets with well-polished edges that are glued together). To control the size of the penumbra the aperture blades are in close proximity to the resist. Precise movement of each L-shaped blade in the  $X'$  and  $Y'$  directions defines the size of the beam spot (Fig. 1). This allows rapid exposure of entire rectangular pattern elements with sizes up to  $500 \times 500 \mu\text{m}$  in one step. By combining different dimensions of the defining aperture with the  $x$  and  $y$  sample movements relative to the beam spot, entire fluidic patterns with large reservoirs and narrow flow channels can be written on large areas in short time (Fig. 1). In addition, the PPAL approach eliminates the need of time consuming beam focusing and beam optimization routines. As the PPAL approach is purely based on shadowcasting, it can be used with accelerators where beam focusing is not straightforward, e.g. for high rigidity MeV heavy ion beams or with cyclotron beams having large divergence. A more detailed technical description of the PPAL system can be found elsewhere [10,11].

To examine the feasibility of the PPAL approach several test patterns were written in PMMA using 56 MeV  $^{14}\text{N}^{3+}$  beam from the Jyväskylä cyclotron and a 3 MeV  $^4\text{He}^{2+}$  beam from a Pelletron accelerator.

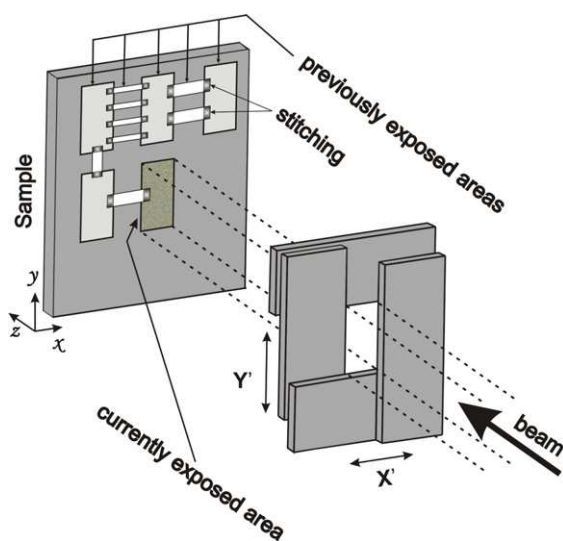


Fig. 1. Schematic illustration of the PPAL system. Two L-shaped aperture blades, each made up of two 100  $\mu\text{m}$  thick Ta sheets glued together, define the beam spot shape and size on the sample. By combining  $X'$  and  $Y'$  of the blades with the  $x$  and  $y$  movement of the sample, entire patterns made up of rectangular structures can be rapidly exposed.

## 2. Experimental procedures

PMMA A11 resist solution was spin-coated on Si substrates at 2500 rpm followed by a soft-bake at 160  $^{\circ}\text{C}$  for 5 min. The procedure was repeated three times to yield a final 7.5  $\mu\text{m}$  resist thickness. The ion beam irradiations were carried out at the Accelerator Laboratory of the Jyväskylä University using the K-130 cyclotron [17] for  $^{14}\text{N}^{3+}$  and the recently commissioned NEC 1.7 MV Tandem Pelletron accelerator for  $^4\text{He}^{2+}$ . Typically 100 nC  $\text{mm}^{-2}$  of 2 MeV protons are required to expose PMMA [18]. Taking into account that the stopping force of 56 MeV  $^{14}\text{N}$  and 3 MeV  $^4\text{He}$  in PMMA is 30 and 8 times larger than that of 2 MeV protons [19], respectively, we estimated that the required fluence is 3.3 particle-nC  $\text{mm}^{-2}$  for  $^{14}\text{N}$  and 12.5 particle-nC  $\text{mm}^{-2}$  for  $^4\text{He}$ . To verify the estimated exposure parameters, a series of lines were written in PMMA with gradually increasing delivered fluences spanning two orders of magnitude. The required exposure fluences appeared to be in good agreement with the previously reported proton fluences [18] taking into account differences in the stopping forces for different ions.

The exposure times were determined by means of a Faraday cup positioned behind the sample holder measuring the current of the beam collimated by  $1 \times 1 \text{mm}^2$  or  $0.5 \times 0.5 \text{mm}^2$  variable aperture openings. To prevent the excessive heating of the computer-controlled aperture by energetic  $^{14}\text{N}$  ions, the  $\sim 9 \text{W}$  cyclotron beam was first collimated by a water-cooled 1 mm diameter Ta aperture located 1.76 m upstream close to the exit of the switching magnet. With close to 500 nA of  $^{14}\text{N}^{3+}$  available at the water-cooled aperture, only  $\sim 100 \text{pA}$  was transported through a  $1 \times 1 \text{mm}^2$  opening of the computer-controlled aperture. With such current densities, approximately 100 s exposure per rectangular pattern element was required. Between the pattern elements exposure the beam was blanked by a TTL signal that gated the cyclotron injection system.

The heating power of 3 MeV  $^4\text{He}$  is much reduced compared to 56 MeV  $^{14}\text{N}$ , therefore the water-cooled aperture was not used when the He irradiations were performed. As one might expect, removing this aperture also increased the available beam current on target. With approximately 20 nA of  $^4\text{He}^{2+}$  measured by a Faraday cup near the exit from the switching magnet of the Pelletron,  $\sim 1\text{--}2 \text{nA}$  are transported through the  $1 \times 1 \text{mm}^2$  opening of the computer-controlled aperture. With such current densities, 15–30 s irradiations per pattern element are sufficient to fully expose PMMA. The beam control between the exposures was realized using an electrostatic two-plate beam blunker positioned downstream from the Faraday cup immediately after the switching magnet. The beam blanking was controlled by a TTL signal fed to a high voltage relay connected to a high voltage supply that applies 1–3 kV to the plates to deflect the beam away from the sample. The apertures and samples stage as well as the the beam blanking were controlled by purpose-built LabView™ software.

Normally, a safety-factor of 50% was added to the exposure times in order to compensate for the beam current and position instabilities. During the exposures the samples were positioned at  $\sim 1$ – $1.5$  mm behind the blade.

After the exposures the samples were developed in IPA:de-ionized water (7:3) solution [20] for 4–6 min followed by rinsing in de-ionized water and dried under helium flow.

### 3. Results and discussion

Fig. 2 shows a test pattern written using the PPAL system with a 56 MeV nitrogen beam. The pattern is made of three large ( $100 \times 100 \mu\text{m}$ ) reservoirs connected by two flow channels ( $12 \mu\text{m}$  and  $30 \mu\text{m}$  wide). This image reveals the limitations of the system. Firstly, the pattern edge quality is clearly sensitive to dust particles adhering to the aperture edges and also the straightness of the aperture blades. In general, the patterns were written with only limited success with nitrogen ions. One problem is that PMMA is sensitive to the nitrogen fluence fluctuations and easily crosslinks in the stitching areas that receive double the fluence (not shown). At low fluences (Fig. 3(a)) the PPAL system can be used to write regions of non-overlapping ion tracks. These could be used as capillary pumps and as filters and permeable membranes in 3D microfluidics circuits. At increasing fluences the ion tracks overlap (Fig. 3(b) and (c)). At still higher fluences, but not so high that the cross-linking occurs, the exposed PMMA is completely removed after development (Fig. 3(b)). It was observed that the pattern-edges were relatively rough (e.g. as compared to He irradiation, below). This may be attributed to the stochastic dose variations close to the edge of the irradiated area as the individual ion tracks have relatively large diameter. The case where the ion tracks overlap is a particularly interesting situation where a “carpet” of fiber-like polymer columns with nanometre dimensions is formed (Fig. 3(c)). These structures have potential application as a substrate for biomimetic studies as they can be coated with signal substances to probe the influence of chemical signalling

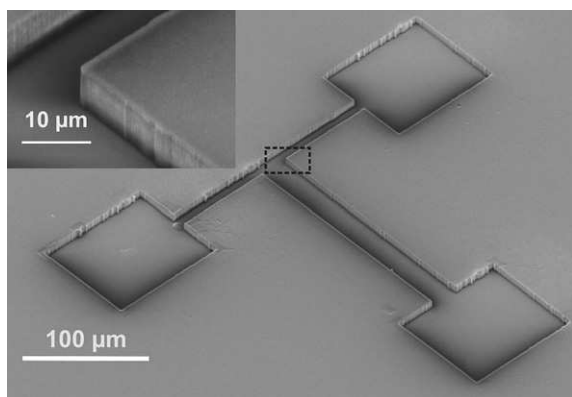


Fig. 2. SEM micrograph of a test pattern produced in a  $7.5 \mu\text{m}$  thick PMMA layer using PPAL system with 56 MeV  $^{14}\text{N}^{3+}$  beam from the Jyväskylä cyclotron (tilt angle  $45^\circ$ ).

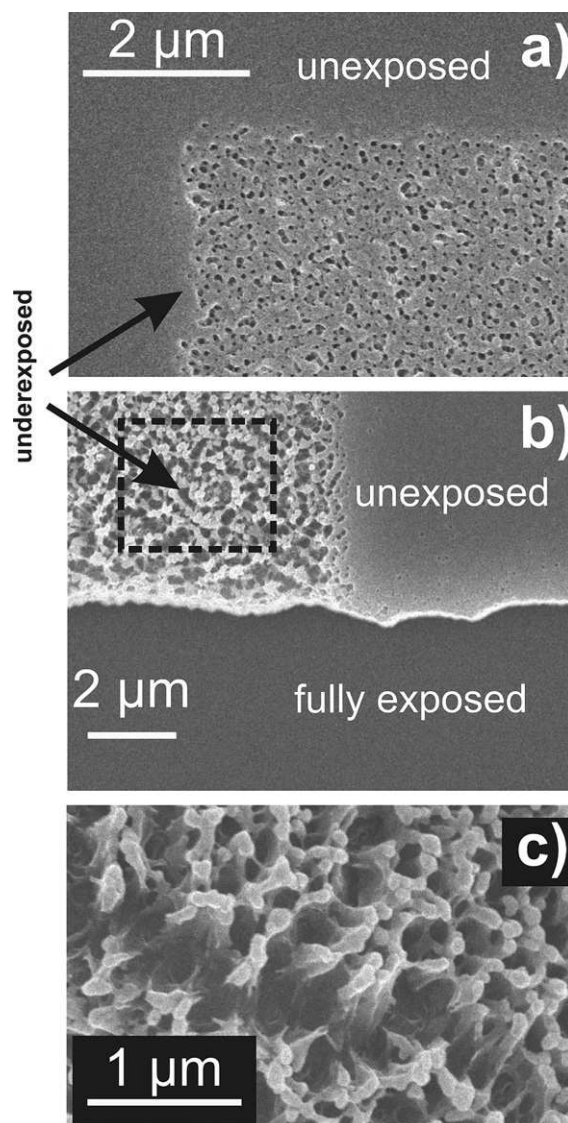


Fig. 3. Illustration of structures formed in PMMA resist by exposure with different fluences of 56 MeV  $^{14}\text{N}^{3+}$  ions. (a) Lithographically defined region of single ion-tracks, (b) higher fluences giving partial overlap of the ion tracks and a fully exposed region and (c) magnified region of the underexposed region in (b).

combined with nanometre-scale topography on cell proliferation.

Fig. 4 illustrates a prototype pattern written using 3 MeV  $^4\text{He}^{2+}$  beam. The pattern consists of five large ( $200 \times 200 \mu\text{m}$ ) reservoirs (not shown) connected through  $30 \mu\text{m}$  wide flow channels to a sorting device illustrated in Fig. 4(a). The sorting device consists of a series of flow channels with decreasing dimensions. Fig. 4(b) shows magnified image of  $22 \mu\text{m}$  and  $12 \mu\text{m}$  wide channels, while Fig. 4(c) and (d) shows  $5 \mu\text{m}$  and  $\sim 1.6 \mu\text{m}$  wide channels, respectively. These  $\sim 1.6 \mu\text{m}$  wide channels are the smallest feature written systematically so far with the PPAL system. One may expect that ions scattered from the aperture edges degrade the sharpness of the pattern in a stochastic way. Aperture edge roughness on the other hand is not stochastic

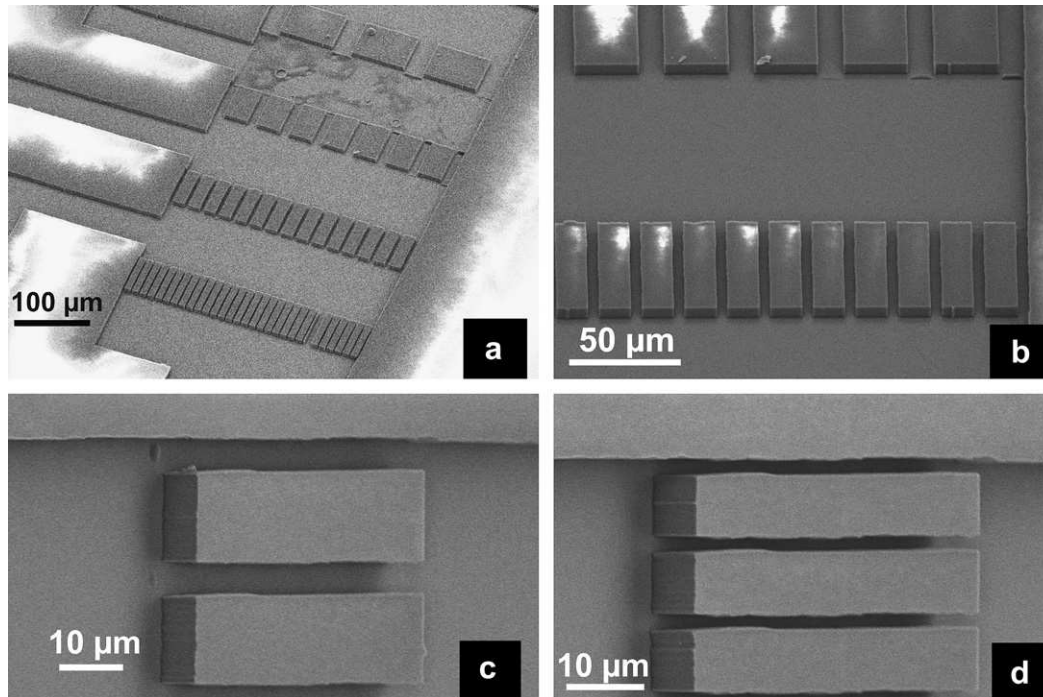


Fig. 4. SEM micrographs of patterns written in 7.5  $\mu\text{m}$  thick PMMA layer using PPAL system with 3 MeV He beam from a Pelletron accelerator, (a) closeup of the sorting device, in the central area of a microfluidic device. The device consists of large  $200 \times 200 \mu\text{m}$  reservoirs (not shown) connected via flow channels to the sorting device that has a series of flow channels with decreasing dimensions, (b) magnified image of the 20  $\mu\text{m}$  and 10  $\mu\text{m}$  wide channels, (c) magnified image of the 5  $\mu\text{m}$  wide channels and (d) magnified image of the 1.5  $\mu\text{m}$  wide channels.

but will follow the departures from perfectly straight aperture edges. Close inspection of Fig. 4(c) and (d) show that the detailed shape of the upper and lower edges of the channels is reproduced for each channel. The major contribution to pattern-edge roughness (the smallest channel mean-width  $d_{\text{mean}} = 1.6 \mu\text{m}$ , minimal width  $d_{\text{min}} = 1.3 \mu\text{m}$ , and maximal width  $d_{\text{max}} = 1.9 \mu\text{m}$ ) can be associated with aperture edge roughness. This is in agreement with the preliminary theoretical study of the ion-scattering by the aperture edges [21] performed using the GEANT4 toolkit [22]. It is then clear that the pattern quality can be further improved by improved polishing of the Ta blade edges, e.g. using sputtering or cluster-ion bombardment [23]. Positioning accuracy of the linear-motion drives [24] is important for obtaining the correct dimensions of the desired structures. To estimate the positioning accuracy, corresponding channel-edge-to-channel-edge distances were measured for the smallest channels. In this case, the standard deviation of the measured distances distribution (0.14  $\mu\text{m}$ ), or the FWHM of the distribution (0.34  $\mu\text{m}$ ), are measures of the positioners accuracy. The measured positioning accuracy is then comparable with the edge-to-edge measurement error ( $\sim 0.3 \mu\text{m}$ ) resulting from an uncertainty in the pattern edge thickness of a few pixels and an uncertainty of the pixel size in the SEM images of the channels.

Sometimes, cross-linked PMMA can be observed in some of the stitching areas, (regions where two rectangular pattern areas are overlapped to prevent unwanted gaps). These can be associated with variations in the beam current

and were particularly prominent in the case of the 56 MeV  $^{14}\text{N}^{3+}$  exposures. This can be corrected by normalising the exposure time for each pattern element according to the beam current (e.g. using a Rutherford backscattering signal, secondary electron signals [25] or ionoluminescence [26]). Likewise, we have observed a tendency for some large pattern elements areas ( $>200 \mu\text{m}$ ) to be exposed non-uniformly. This could be attributed to beam spot inhomogeneity. A simple correction for this is by de-focussing the beam albeit at the expense of increasing the exposure times.

#### 4. Conclusions

Test microfluidic patterns were fabricated in thick PMMA using a novel approach of MeV ion beam Programmable Proximity Aperture Lithography (PPAL). The patterns exhibit sharp edges, straight and relatively smooth walls thus proving the feasibility of the PPAL approach with MeV ions. The minimal size structure systematically written with the system is 1.5  $\mu\text{m}$  at the moment, which can be further improved. The system can also be used to lithographically define regions of ion tracks having features with nanometre dimensions, which may be useful in biomedical and cellular studies.

#### Acknowledgements

This work has been carried out under the auspices of the Academy of Finland Centre of Excellence in Nuclear and

Accelerator Based Physics (Ref. 213503) and the BOGOTAS consortium. SG is grateful for travel support from the Graduate School of Particle and Nuclear Physics. Professors Matti Vuento and Frank Watt, as well as Andrew Bettiol and Jeroen van Kan are warmly thanked for helpful discussions and advise.

## References

- [1] M. Yoshida, K. Tohda, M. Gratzl, *Anal. Chem.* 75 (2003) 4686.
- [2] P.S. Dittrich, P. Schwille, *Anal. Chem.* 75 (2003) 5767.
- [3] Y. Huang, N.S. Sekhlon, J. Borninski, N. Chen, B. Rubinsky, *Sensors Actuat. A* 105 (2003) 31.
- [4] M. Foquet, J. Korlach, W. Zipfel, W.W. Webb, H.G. Craighead, *Anal. Chem.* 74 (2002) 1415.
- [5] H.-P. Chou, C. Spence, A. Scherer, S. Quake, *Proc. Natl. Acad. Sci. USA* 96 (1999) 11.
- [6] A. van Orden, H. Cai, P.M. Goodwin, R.A. Keller, *Anal. Chem.* 71 (1999) 2108.
- [7] T. Vilkner, D. Janasek, A. Manz, *Anal. Chem.* 76 (2004) 3373.
- [8] E. Delamarche, D. Juncker, H. Schmidt, *Adv. Mater.* 17 (2005) 2911.
- [9] S. Gorelick, P. Rahkila, A. Sagari A.R., T. Sajavaara, S. Cheng, L.B. Karlsson, J.A. van Kan, H.J. Whitlow, *Nucl. Instr. and Meth. B* 260 (2007) 130.
- [10] S. Gorelick, T. Ylimäki, T. Sajavaara, M. Laitinen, A. Sagari A.R., H.J. Whitlow, *Nucl. Instr. and Meth. B* 206 (2007) 77.
- [11] N. Puttaraksa, S. Gorelick, T. Sajavaara, M. Laitinen, S. Singkarat, H.J. Whitlow, Programmable proximity aperture lithography with MeV ion, *J. Vac. Sci. Technol. B* (2008), submitted for publication.
- [12] F. Watt, M.B.H. Breese, A.A. Bettiol, J.A. van Kan, *Mater. Today* 30 (2007) 20.
- [13] J.A. van Kan, A.A. Bettiol, F. Watt, *Nucl. Instr. and Meth. B* 260 (2007) 396.
- [14] S.Y. Chiam, J.A. van Kan, T. Osipowicz, C.N.B. Udalagama, F. Watt, *Nucl. Instr. and Meth. B* 260 (2007) 455.
- [15] J. van Erps, B. Volckaerts, H. van Amerongen, P. Vynck, R. Krajewski, C. Debaes, J. Watte, A. Hermanne, H. Thienpont, *IEEE Photon. Technol. Lett.* 18 (2006) 1164.
- [16] M.L. Taylor, A. Alves, P. Reichart, R.D. Franich, S. Rubanov, P. Johnston, D.N. Jamieson, *Nucl. Instr. and Meth. B* 260 (2007) 426.
- [17] E. Liukkonen, et al., in: *Proceedings of the 13th International Conference on Cyclotrons and their Applications*, Vancouver, 1992, p. 22.
- [18] J.A. van Kan, J.L. Sanchez, B. Xu, T. Osipowicz, F. Watt, *Nucl. Instr. and Meth. B* 158 (1999) 179.
- [19] J.F. Ziegler, SRIM–2006. Available from: <<http://www.SRIM.org>>.
- [20] S. Yasin, D.G. Hasko, H. Ahmed, *Microelectr. Eng.* 61–62 (2002) 745.
- [21] S. Gorelick, T. Sajavaara, M. Laitinen, N. Puttaraksa, H.J. Whitlow, *Mater. Res. Soc. Symp. Proc.* 1020 (2007) 67.
- [22] S. Agostinelli et al., *Nucl. Instr. and Meth. A* 506 (2003) 250. Available from: <<http://geant4.web.cern.ch/geant4>> .
- [23] I. Yamada, *Nucl. Instr. and Meth. B* 257 (2007) 632.
- [24] Newport ESP300 1–3 Axis Motion Controller/Driver, MFA-CCV6 Miniature Linear Stages. <<http://www.newport.com>>.
- [25] A.A. Bettiol, I. Rajta, E.J. Teo, J.A. van Kan, F. Watt, *Nucl. Instr. and Meth. B* 190 (2002) 154.
- [26] C.N.B. Udalagama, A.A. Bettiol, J.A. van Kan, F. Watt, *Nucl. Instr. and Meth. B* 210 (2003) 256.